Fish and Shellfish Immunology 88 (2019) 556–566

Contents lists available at ScienceDirect

Fish and Shellfish Immunology

journal homepage: www.elsevier.com/locate/fsi

Full length article

Molecular cloning and characterization of FADD from the manila clam *Ruditapes philippinarum*

Gege Hu[a,d], Yijing Han[a,d], Dinglong Yang[a,b,**], Ruiwen Cao[a,d], Qing Wang[a,b], Hui Liu[a,b], Zhijun Dong[a,b], Xiaoli Zhang[a,b], Qianqian Zhang[a,b], Jianmin Zhao[a,b,c,*]

[a] *Muping Coastal Environment Research Station, Yantai Institute of Coastal Zone Research, Chinese Academy of Sciences, Yantai, 264003, PR China*
[b] *Research and Development Center for Efficient Utilization of Coastal Bioresources, Yantai Institute of Coastal Zone Research, Chinese Academy of Sciences, Yantai, 264003, PR China*
[c] *Center for Ocean Mega-science, Chinese Academy of Sciences, Qingdao, Shandong, 266071, PR China*
[d] *University of Chinese Academy of Sciences, Beijing, 100049, PR China*

ARTICLE INFO

Keywords:
FADD
Ruditapes philippinarum
NF-κB
Apoptosis

ABSTRACT

Fas-associated protein with death domain (FADD) is an essential element in cell death, and also implicates in cell cycle progression, inflammation and innate immunity. In the study, an FADD (designated as RpFADD) was identified and characterized from manila clam, *Ruditapes philippinarum*. Multiple alignments and phylogenetic analysis strongly suggested that RpFADD was a new member of the FADD family. The RpFADD transcripts were constitutively expressed in a wide range of tissues, and dominantly expressed in hemocytes. After challenged with *Vibrio anguillarum* or *Micrococcus luteus*, the expression level of RpFADD transcripts was significantly induced and reached the maximum level at 72 h and 48 h, respectively. Knockdown of RpFADD down-regulated the transcript levels of RpIKK, RpTAK1 and RpNF-κB with the exception of RpIκB. Moreover, RpFADD primarily localized in the cell cytoplasm, and its over-expression promoted the apoptosis of HeLa cells. These results revealed that RpFADD perhaps regulated the NF-κB signaling pathways positively, which provided a better understanding of RpFADD in innate immunity.

1. Introduction

Apoptosis is a highly regulated and conserved form of active cell death. In receptor-mediated apoptosis, it is produced by the activation of a protein-signaling complex that involves the physical association of caspases [1]. Fas binding to Fas-associated protein with death domain (FADD) activate FADD-caspase-8 binding to form death-inducing signaling complex (DISC). DISC eventually leads to cleavage of downstream targets and apoptosis [2]. As a proapoptotic adaptor molecule, FADD is composed of the N-terminal death effector domain (DED) and the C-terminal death domain (DD). Its C-terminal domain has been proposed as a putative third functional domain, which contains an important single phosphorylation site in a serine-rich region [3,4]. Both DED and DD adopt a six α-helical bundle structure that is characteristic of a structural family of "death motifs". The DD is engaged with receptor, while the DED contains the binding site for procaspase-8 and -10 [5–7].

In recent years, some alternative functions of FADD have been reported in invertebrates and vertebrates. Usually, FADD not only causes apoptosis and cell proliferation defects, but also participates in a variety of non-apoptotic processes, such as innate immune signaling, hematopoiesis, cell cycle regulation and embryogenesis [8]. In mammals, FADD was activated to assemble DISC with Fas and procaspases-8 and -10 after death receptors engaging ligands. Then procaspase-8 undergoes auto-processing, becomes activated and cleaves downstream effector caspases or the protein bid leading to cell death [9]. In *Drosophila*, this same complex includes FADD and a caspase homologue, Dredd. They regulated apoptosis and antimicrobial responses by producing a wide range of potent antimicrobial peptides in response to fungi or bacteria [10,11].

Ruditapes philippinarum is an economic species widely spread over many countries. Recent mass mortalities in manila clams have been

* Corresponding author. Muping Coastal Environment Research Station, Yantai Institute of Coastal Zone Research, Chinese Academy of Sciences, Yantai, 264003, PR China.
** Corresponding author. Muping Coastal Environment Research Station, Yantai Institute of Coastal Zone Research, Chinese Academy of Sciences, Yantai, 264003, PR China.
E-mail addresses: dlyang@yic.ac.cn (D. Yang), jmzhao@yic.ac.cn (J. Zhao).

https://doi.org/10.1016/j.fsi.2019.03.033
Received 25 January 2019; Received in revised form 12 March 2019; Accepted 13 March 2019
Available online 16 March 2019
1050-4648/

Table 1
Primers used in the present study.

Primer	Sequence (5′-3′)	Sequence information
P1	AATTCCTACAAAGACATGCT	3′ RACE primer
P2	GCAATTCGAGCACTTGAAAAT	3′ RACE primer
P3	GGACCACAGACTCAAACACCACC	Real-time PCR
P4	TGAGTATTGGTTATCCCATCAGGT	Real-time PCR
P5	ACGAGGACGTAGCTGCTTTGGT	β-actin primer
P6	CCGATAGTGATGACCTGACC	β-actin primer
P7	CTTGGATCCATGGACGAGCGTCATAATTCCT	Recombinant primer
P8	CGCGAATTCTCAATATCTGCCCTCCTCTAAC	Recombinant primer
P9	TAATACGACTCACTATAGGGATCATGGACGAGCGTCATAATTCC	dsRpFADD primer
P10	TAATACGACTCACTATAGGGATCAACATAAACAATCTGTTGTCCT	dsRpFADD primer
P11	TAATACGACTCACTATAGGGATCCGACGTAAACGGCCACAAGT	dsGFP primer
P12	TAATACGACTCACTATAGGGATCCTTGTACAGCTCGTCCATGC	dsGFP primer
P13	GCCCGTCCAATGGCATAAAGAA	Real-time PCR
P14	TTCCGCAACCACTGTTCAAGGT	Real-time PCR
P15	TCAGTTCGTGTTTACCCAATGCC	Real-time PCR
P16	GCCGTAATCTGTCCCGTACTTCC	Real-time PCR
P17	GGCAAACTGAAATTGTGAAAGCT	Real-time PCR
P18	TTCGTCCAGATACATCGTCACCAAA	Real-time PCR
P19	GCAGATCAGTGCTCTTCAGGGAC	Real-time PCR
P20	TGAACCACCATCTTCTTCCAAAT	Real-time PCR
P21	GAAAATGAGGACGATGATTGCTT	Real-time PCR
P22	TTCACAATAGCCTTCCCTACAAC	Real-time PCR
P23	TGGTCGTCGTGCCAAGACAAAT	Real-time PCR
P24	TCCCGAACTACCGCTACCTCAA	Real-time PCR
d_T	GGCCACGCGTCGACTAGTACT$_{17}$	Oligo (d_T)-adaptor

attributed to pathogen invasion and environmental deterioration. Therefore, it is urgently necessary to characterize the immune-regulated molecules for diseases control. Recently, studies on the immune function of FADD only appear in several members of vertebrates [12–14] and insects [15]. However, basic knowledge of signal conduction of FADD is still lacking in marine mollusks. In the present study, a FADD gene was identified and characterized from *Ruditapes philippinarum* (designated as RpFADD), and the temporal and spatial expression of RpFADD was also investigated. Meanwhile, regulation of RpFADD on NF-κB signal pathway and several immune-related genes was analyzed. In addition, the intercellular localization of RpFADD was detected, and its roles of regulating apoptosis were examined in FADD-transfected HeLa cells.

2. Materials and methods

2.1. Clam culture, bacterial challenge and tissues collection

Healthy manila clams (shell length of 3.0–4.0 cm) were purchased from a local culture farm in Yantai, Shandong Province, China, and acclimatized in the aerated seawater at 20–22 °C for 10 days before processing. The clams were fed with an algae mixture of *Isochrysis galbana* and *Phaeodactylum tricornutum*. The seawater was totally renewed daily.

In order to determine the tissue expression profiles of RpFADD, several tissues, including gills, hemocytes, hepatopancreas, mantle and muscle were collected from six healthy clams. Then, three hundred clams were employed for the bacterial stimulation experiment. The clams were randomly divided into three groups and kept in nine aerated tanks (50 L). Three tanks served as the control, while the other six tanks were immersed with *V. anguillarum* or *M. luteus* at a final concentration of 1×10^7 CFU mL^{-1}, respectively. The hemocytes of six individuals were randomly sampled at 0, 3, 6, 12, 24, 48 and 72 h post bacterial challenge.

2.2. Gene cloning and sequence analysis

Total RNA was extracted using Trizol reagent according to the manufacture's protocol (Invitrogen) [16]. The purified RNA was digested with DNase I (Invitrogen, amplification grade) to remove possible genomic DNA contamination. Furthermore, the first-strand cDNA was synthesized with M-MLV reverse transcriptase (Promega, USA).

A manila clam EST was identified through large-scale EST sequencing of the constructed cDNA library. Nested-PCR was performed with P1, P2 as forward primers (Table 1) and oligo (d_T) as reverse primer to amplify the 3' end of RpFADD. The full-length cDNA of RpFADD was obtained by overlapping the original EST sequence and the amplified fragments.

The nucleotide sequence and deduced amino acid analysis were performed using the BLAST algorithm at NCBI website (http://www.ncbi.nlm.nih.gov/blast), and the Expert Protein Analysis System (http://www.expasy.org/). Multiple alignments were performed with the ClustalW Multiple Alignment program and Multiple Alignment Show program. A neighbor-joining phylogenetic tree of FADDs was constructed by MEGA 4.1 with 1000 bootstrap replicates.

2.3. Spatial and temporal expression of RpFADD transcripts

The qRT-PCR was performed using Applied Biosystems 7500 fast Real-Time PCR System (Applied Biosystems, USA) to determine tissue specific and temporal expression of RpFADD. Gene-specific primers (P3 and P4, Table 1) and β-actin primers (P5 and P6, Table 1) were used to

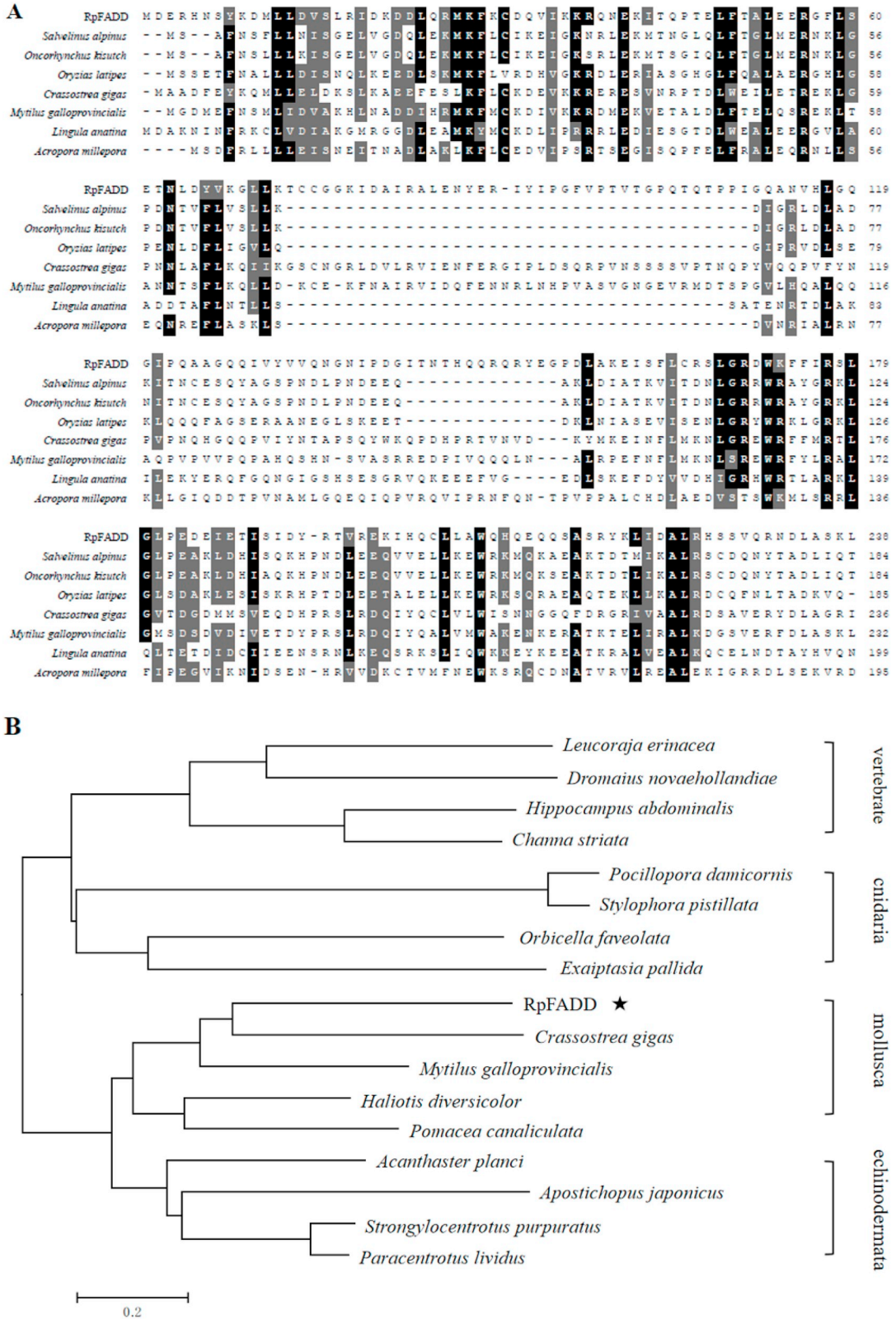

Fig. 1. Molecular cloning of RpFADD. (A) Multiple sequence alignments of FADDs. Comparison of RpFADD with FADDs from living creature, including *Crassostrea gigas* (AEB54797); *Mytilus galloprovincialis* (AHI17305); *Acropora millepora* (AJG36592); *Lingula anatina* (XP_013392457); *Oryzias latipes* (NP_001098257); *Salvelinus alpinus* (XP_023858848) and *Oncorhynchus kisutch* (XP_020333161). Identical residues are marked in dark, and similar amino acids are shaded in gray. (B) A phylogenetic tree constructed by the neighbor-joining method based on amino acid sequences of FADDs. The protein sequences used for the phylogenetic tree are listed as follows: *Crassostrea gigas* (EKC21432); *Mytilus galloprovincialis* (AHI17305); *Pomacea canaliculata* (PVD39589); *Haliotis diversicolor* (AOW44266); *Pocillopora damicornis* (XP_027045189); *Stylophora pistillata* (XP_022805150); *Orbicella faveolata* (XP_020628669); *Exaiptasia pallida* (KXJ14990); *Apostichopus japonicus* (PIK53982); *Strongylocentrotus purpuratus* (XP_791975); *Paracentrotus lividus* (ABQ51094); *Acanthaster planci* (XP_022087555); *Leucoraja erinacea* (ACH96579); *Hippocampus abdominalis* (AMA01983); *Dromaius novaehollandiae* (XP_025964762) and *Channa striata* (CCV01626).

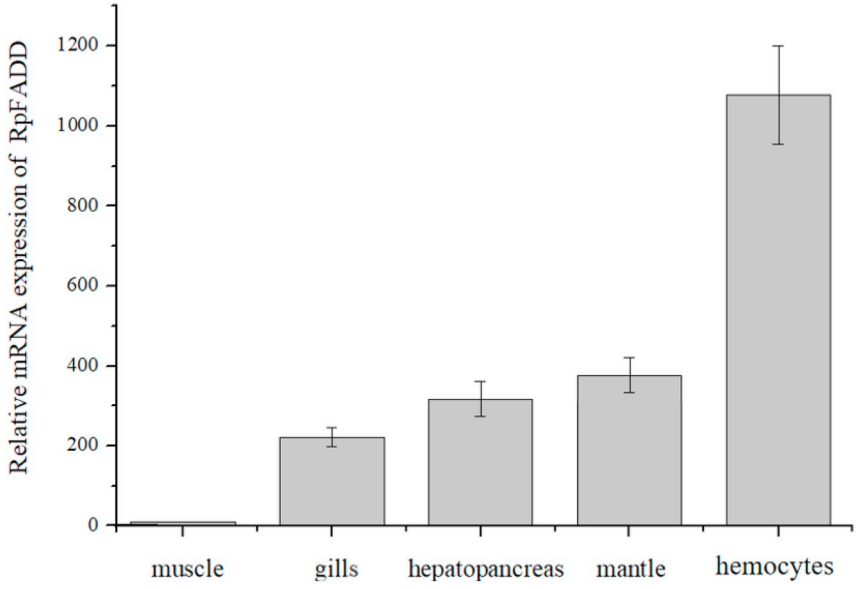

Fig. 2. The expression of RpFADD mRNA in different tissues of clams detected by qRT-PCR. Transcript levels in mantle, gills, hemocytes and hepatopancreas are normalized to that of muscle. Vertical bars represent the mean ± S.D. (N = 6).

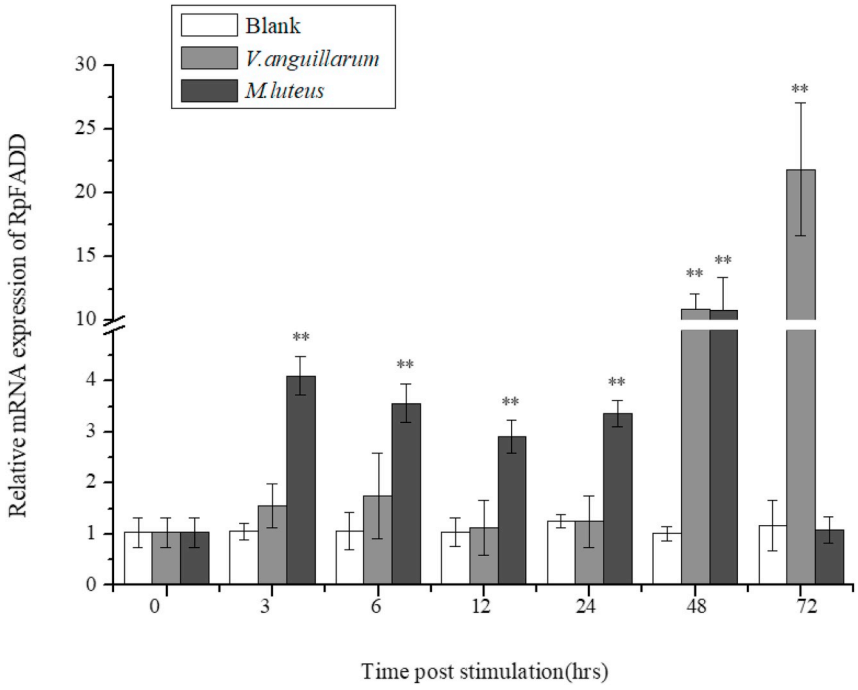

Fig. 3. Temporal expression profiles of RpFADD mRNA in hemocytes of clams post *V. anguillarum* or *M. luteus* challenge. The values are shown as mean ± S.D. (N = 6) (*: $P < 0.05$, **: $P < 0.01$).

amplify the fragments of RpFADD and internal control, respectively. The purity of amplification products was evaluated by dissociation curve analysis. The $2^{-\triangle\triangle CT}$ method was used to analyze the relative expression level of RpFADD [17]. All data were given in terms of relative mRNA expressed as mean ± S.D. (N = 6).

2.4. Recombinant expression of RpFADD

The open reading frame (ORF) of RpFADD was amplified with primes P7 and P8 (Table 1), and sub-cloned into the expression vector pEASY-E1 (Transgen, China) to construct prokaryotic expression

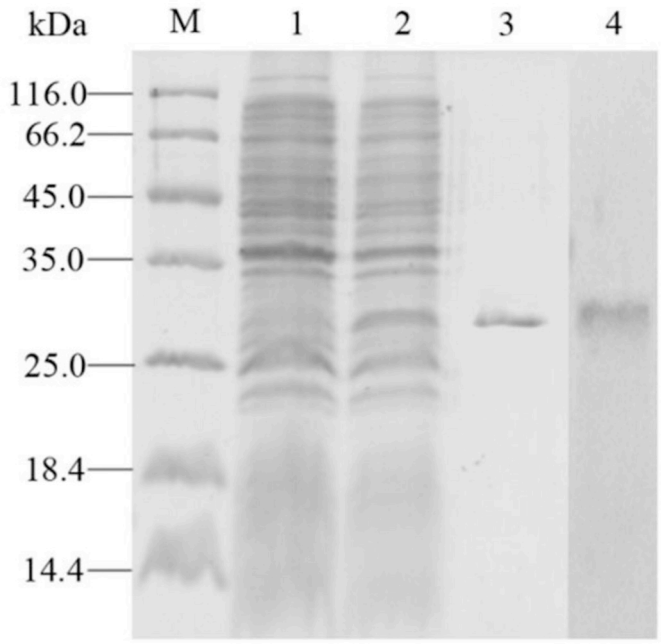

Fig. 4. SDS-PAGE analysis of recombinant RpFADD. Lane M: protein molecular standard; lane 1: uninduced bacterial lysate; lane 2: bacterial lysate after induction with IPTG; lane 3: purified rRpFADD; lane 4: western blotting analysis of RpFADD.

plasmid. The positive recombinant plasmids were transformed into compete *Escheichia coli* BL21 (DE3) to express the fusion recombinant RpFADD protein (rRpFADD). The rRpFADD were purified on a Ni^{2+} chelating sepharose column, refolded in gradient urea-TBS glycerol buffer, and verified by 15% SDS-polyacrylamide gel electrophoresis (SDS-PAGE).

2.5. Generation of polyclonal antibodies and western blotting analysis

The rRpFADD with complete Freund's adjuvant (Sigma, USA) were immunized into six-week-old male mice (LuYe Pharma, China) to produce antibodies. The mice were intraperitoneally injected with 100 μg rRpFADD with complete Freund's adjuvant (Sigma, USA) each. Seven days after the initial injection, the mice received another injection in subcutaneous with the same dose antigen emulsified in incomplete Freund's adjuvant, and double injection in caudal vein with the same dose antigen emulsified in incomplete Freund's adjuvant with a 7-days interval between the injections. Seven days after the last injection, the immunized mice were sacrificed and the serum was collected.

Western blotting analysis was used to test the specificity of the antibodies. The total proteins were separated by SDS-PAGE in 15% gels and transferred onto PVDF membranes by electroblotting at 100 V for 1.5 h. The membranes were blocked with 5% non-fat dry milk at 37 °C for 1 h, and then probed with diluted mice anti-rRpFADD (1:3000) antibodies at 4 °C overnight. After washed three times in PBS containing 0.1% Tween-20 (PBS-T), the membranes were incubated with a 1:5000 diluted AP-conjugated goat anti-mouse IgG antibody (Beyotime, China) in PBS at 37 °C for 1 h. Protein bands were stained with freshly prepared substrate solution BCIP/NBT Chromogen Kit (Solarbio, China) for 15 min after the final wash. Pre-immune serum was used as negative control.

2.6. Synthesis and microinjection of dsRNA

The dsRNA templates of FADD and GFP (as control) were amplified using primer P9, P10 and P11, P12 (Table 1). Products with a T7 promoter were confirmed via sequencing. Furthermore, the products were used as templates to produce the sense and antisense RNA strands, subjected to in vitro transcription, and then purified using the RiboMAXTM Large-Scale RNA production System-T7 (Promega, USA) according to the manufacturer's protocol. Finally, the dsRNA was dissolved in RNase-free water to a final concentration of 1 mg/mL.

2.7. The regulation of NF-κB signaling pathway and immune-related genes

Gene knockdowns were performed by injecting 500 ng respective dsRNA into the adductor of the clam *in vivo*. Six clams in the experimental group were injected with dsRpFADD and the control group was injected with dsGFP or PBS. Clams without injection were used as blanks. At 72 h after injection, hemocytes were extracted from 6 individuals to examine the gene silencing efficiency using qRT-PCR and western blotting analysis. Meanwhile, hemocytes were sampled at 0, 12, 24, 48 and 72 h post-dsRNA injection to analyze expression levels of NF-κB signaling pathway (P13, P14 for RpIKK, P15, P16 for RpTAK1, P17, P18 for RpIκB, P19, P20 for RpNF-κB, Table 1) and immune-related genes (P21, P22 for RpDefensin and P23, P24 for RpMacin, Table 1) by qRT-PCR. To ensure the regulatory mechanism of RpFADD, individuals were treated with dsRpFADD or dsGFP and then stimulated with *V. anguillarum* or *M. luteus*, respectively. Clams without injection were used as blanks. At 72 h, hemocytes were collected to analyze expression levels of NF-κB signaling pathway and immune-related genes by qRT-PCR as described above.

2.8. Construction of recombinant plasmid

The complete cDNA fragment of the RpFADD gene was amplified using the primers P7 and P8 (Table 1) with *Bam*H I and *Eco*R I (NEB, USA) site sequences added to their 5' end, respectively. The PCR products were then subcloned into the mammalian expression vector pcDNA3.1/EGFP (Clontech, USA). The pcDNA3.1/EGFP vector containing the RpFADD sequence was constructed into the *Bam*H I and *Eco*R I double digested sites of the vector. The recombinant plasmids (pcDNA3.1/EGFP-RpFADD) and empty plasmid (pcDNA3.1/EGFP-N1) were transformed into *E. coli* DH5α (Tiangen, China) for sequencing, respectively. Then these plasmids were extracted with an EndoFree plasmid mini kit II (Omega, USA).

2.9. Cell culture and transfection

HeLa cells (ATCC, Manassas, VA) were maintained in a 3:1 mix of DMEM: F12, 10% FBS with 100 units/mL penicillin and 100 μg/mL streptomycin. HeLa cells were seeded in six-well plates (2×10^5 cells/well) one day before transfection. The transfection was performed with the plasmids: pcDNA3.1/EGFP-RpFADD and the empty vector. The cells were grown to 80% confluence in 6-well plates and then transfected with the indicated plasmids using the Effectene Transfection Reagent (QIAGEN, USA) according to the manufacturer's instructions.

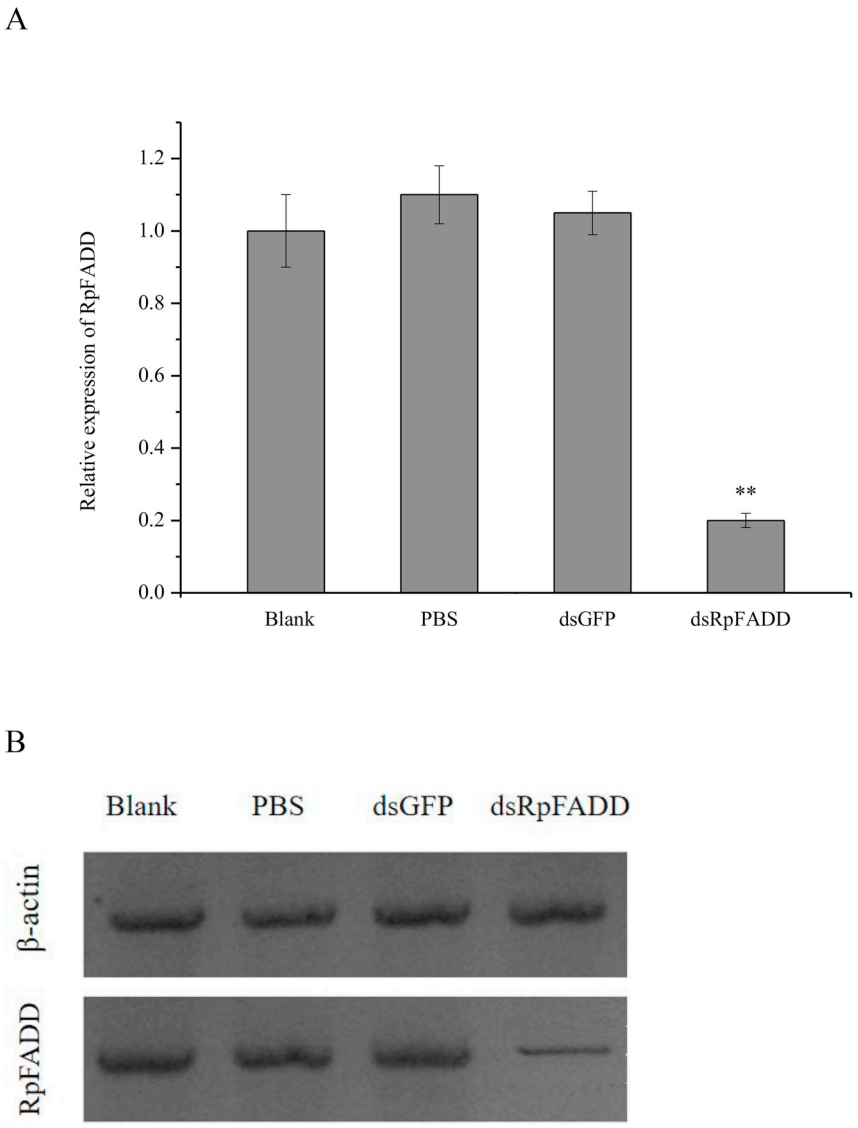

Fig. 5. Evaluation of the silencing efficiency of RpFADD in hemocytes. (A) *R. philippinarum* are injected with dsRpFADD, dsGFP or PBS for 72 h at a final concentration of 100 nM. The relative RpFADD gene expression levels are determined by qRT-PCR. The β-actin gene is used as an internal control to calibrate the cDNA template for all of the samples. The values are shown as mean ± S.D. (N = 6) (*: $P < 0.05$, **: $P < 0.01$). (B) Western blotting analysis of RpFADD in hemocytes.

2.10. Confocal microscopy and apoptosis analysis

For the visualization of subcellular location, HeLa cells were cultured and transfected with target or control plasmid, as described above. Cells were washed twice with PBS at 24 h post-transfection and the nucleus were stained using a 2 mg/mL solution of DAPI (Invitrogen) in PBS at 37 °C for 10 min. The cells were then rinsed twice with PBS and directly observed under fluorescent microscopy (Leica, Germany). Furthermore, the apoptosis rate of HeLa cells was analyzed by flow cytometry accordance with the protocol of Annexin/propidium staining [18]. In brief, the HeLa cells were re-suspended in PBS and 5 μL Annexin-V/FITC (Dojindo, Kumamoto, Japan) and 5 μL PI (50 μg/mL, Dojindo, Kumamoto, Japan) in dark at room temperature for 15 min. After that, the cells were centrifuged for 5 min at 1000 r/min and the pellets were re-suspended by using PBS buffer. Finally, the percentage of apoptotic cells was evaluated by using the flow cytometry (FACSCalibur, BD Biosciences) within 1 h after the Annexin-V/PI staining.

2.11. Statistical analysis

Statistical analysis was performed by one-way analysis of variance (one-way ANOVA) followed by a Duncan test using SPSS 16.0 software, and *P* values less than 0.05 were considered statistically significant.

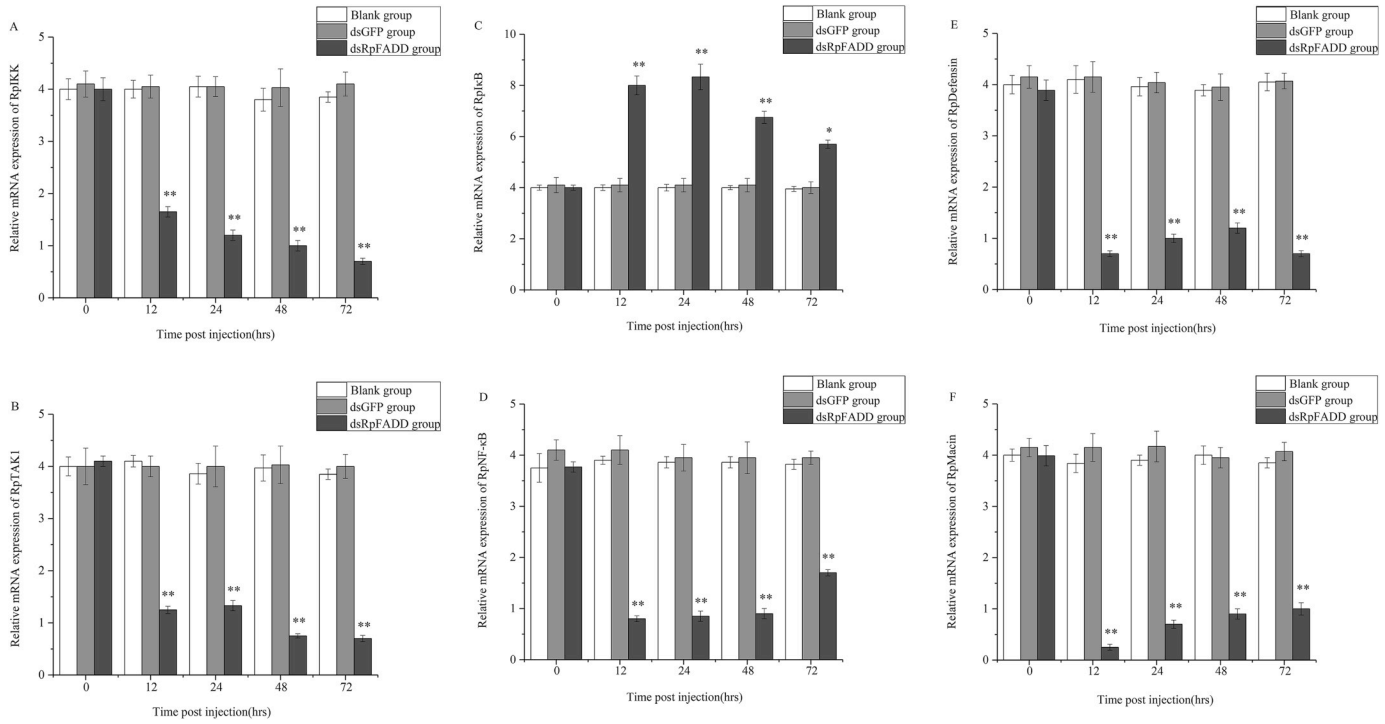

Fig. 6. The relative gene expression levels were determined by qRT-PCR. Time course investigation of quantitative relative mRNA expression of RpIKK (A), RpTAK1 (B), RpIκB (C), RpNF-κB (D), RpDefensin (E) and RpMacin (F) in *R. philippinarum* during RNAi. The β-actin gene is used as an internal control to calibrate the cDNA template for all of the samples. The values are shown as mean ± S.D. (N = 6) (*: $P < 0.05$, **: $P < 0.01$).

3. Results and discussion

3.1. Sequence analysis of RpFADD

In this study, the full-length cDNA of RpFADD was deposited into the GenBank database under the accession number MK422545. The open reading frame (ORF) of RpFADD was of 732 bp, and encoded a polypeptide 243 amino acids long, with an isoelectric point of 7.01 and a predicted molecular weight of 27.9 kDa. Blast analysis revealed significant sequence similarity of RpFADD with other FADDs. For example, RpFADD shared 32% identity from *Crassostrea gigas* (NP_001295786), and 33% identity from *Mytilus galloprovincialis* (AHI17305) (Fig. 1A). A phylogenetic tree was constructed using neighbor-joining method based on the multiple alignments of RpFADD and other known FADDs. The phylogenetic analysis showed that these sequences of RpFADD were split into four groups, including mollusca, echinodermata, cnidaria and vertebrate clades (Fig. 1B). These results indicated that RpFADD is a new member of the FADD family.

3.2. Tissue distribution of RpFADD

Quantitative real-time PCR analysis was employed to determine the tissue-specific expression of the RpFADD transcript. FADD is fairly well documented involvement in developmental processes and immune tissues [15]. In support of the latter role, we observed that RpFADD mRNA transcripts were predominantly expressed in hemocytes, moderately in hepatopancreas, mantle and gills, and marginally expressed in muscle (Fig. 2). Usually, hemolymph carries immune cells and bioactive molecules specialized in pleiotropic defenses against pathogens, which may result in a prior immune response to bacterial challenge in hemocytes than gills and hepatopancreas [19]. Similarly, in mosquito, transcript levels of AeFADD were dominantly expressed in gut and fat body tissues, both of which have high cell turnover rates and are immune-competent tissues known to express AMPs [15].

3.3. Temporal expression profiles of RpFADD after M. luteus or V. anguillarum challenge

Fig. 3 depicted the expression profiles of RpFADD mRNA in hemocytes after *V. anguillarum* or *M. luteus* challenge. The mRNA expression of RpFADD reached the maximum value (7.3-fold, $P < 0.01$) at 48 h in hemocytes post *M. luteus* challenge. After that, the expression level of RpFADD was down-regulated to the original level at 72 h post challenge. After *V. anguillarum* challenge, the mRNA expression level of RpFADD was significantly up-regulated at 48 h (10.1-fold, $P < 0.01$) and 72 h (21.4-fold, $P < 0.01$). These results indicated that RpFADD might be involved in innate immune responses of manila clams. Different from the present study, FADD expression in *Aedes aegypti* was up-regulated four-fold in response to *E. coli* challenge, but no significant changes in response to *M. luteus* stimulation was observed [15]. These

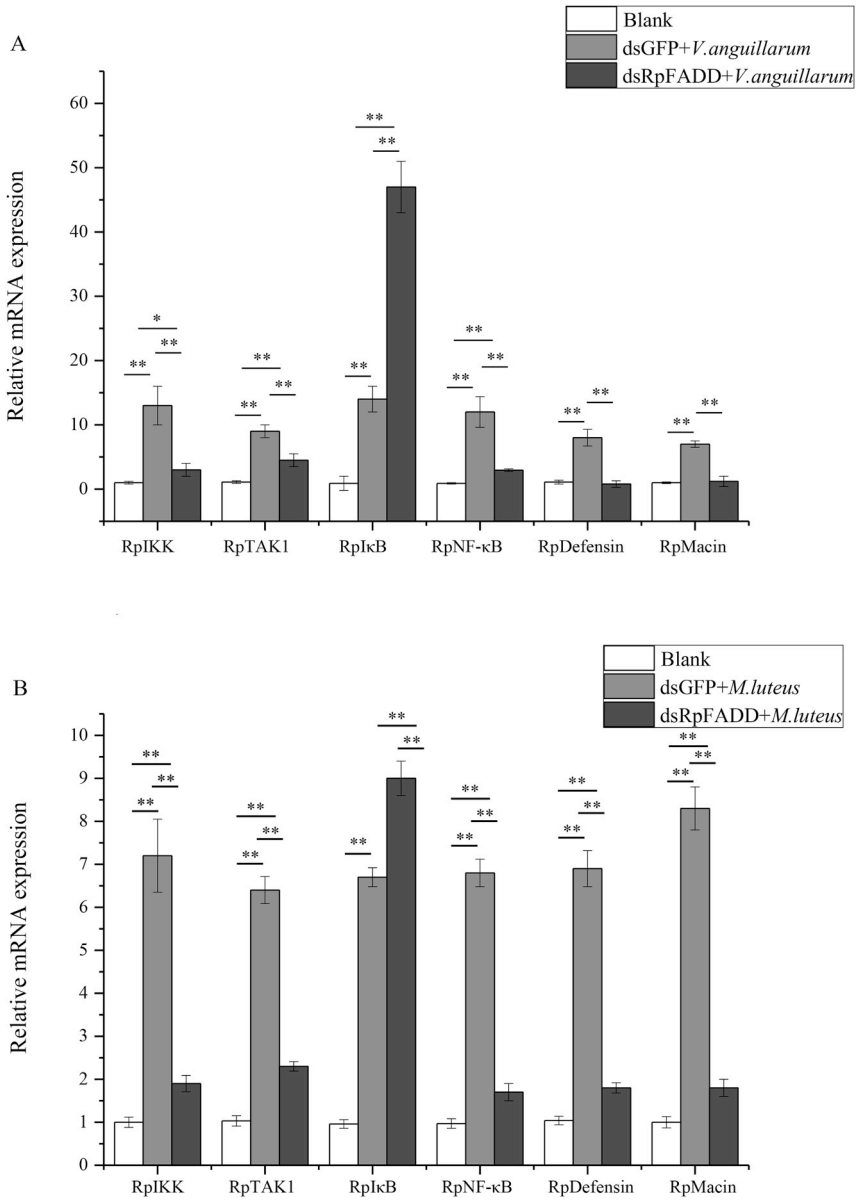

Fig. 7. Down-regulation of RpFADD expression regulates the downstream gene expression in *R. philippinarum* challenged with *V. anguillarum* (A) or *M. luteus* (B). The β-actin gene is used as an internal control to calibrate the cDNA template for all of the samples. The values are shown as mean ± S.D. (N = 6) (*: $P < 0.05$, **: $P < 0.01$).

differences perhaps indicated different roles of FADD involved in the signaling pathways between the insects and mollusks.

3.4. Recombinant production of RpFADD

The recombinant RpFADD were highly expressed in *E. coli* BL21 (DE3) after induction by IPTG. A single band with a molecular mass about 28 kDa was identified (Fig. 4), which was consistent with the expected MW of the mature protein. The recombined proteins incubated with the corresponding antibodies showed only one band on the PVDF membrane, indicating the specificity of these antibodies (Fig. 4).

3.5. The regulatory activity of RpFADD

To evaluate whether RpFADD could activate downstream NF-κB signaling and immune-related genes in *R. philippinarum*, we knocked down the RpFADD gene by RNA interference. Then its expression level was analyzed to validate the silencing efficiency in *R. philippinarum* hemocytes. As shown in Fig. 5A, there is no significant difference in

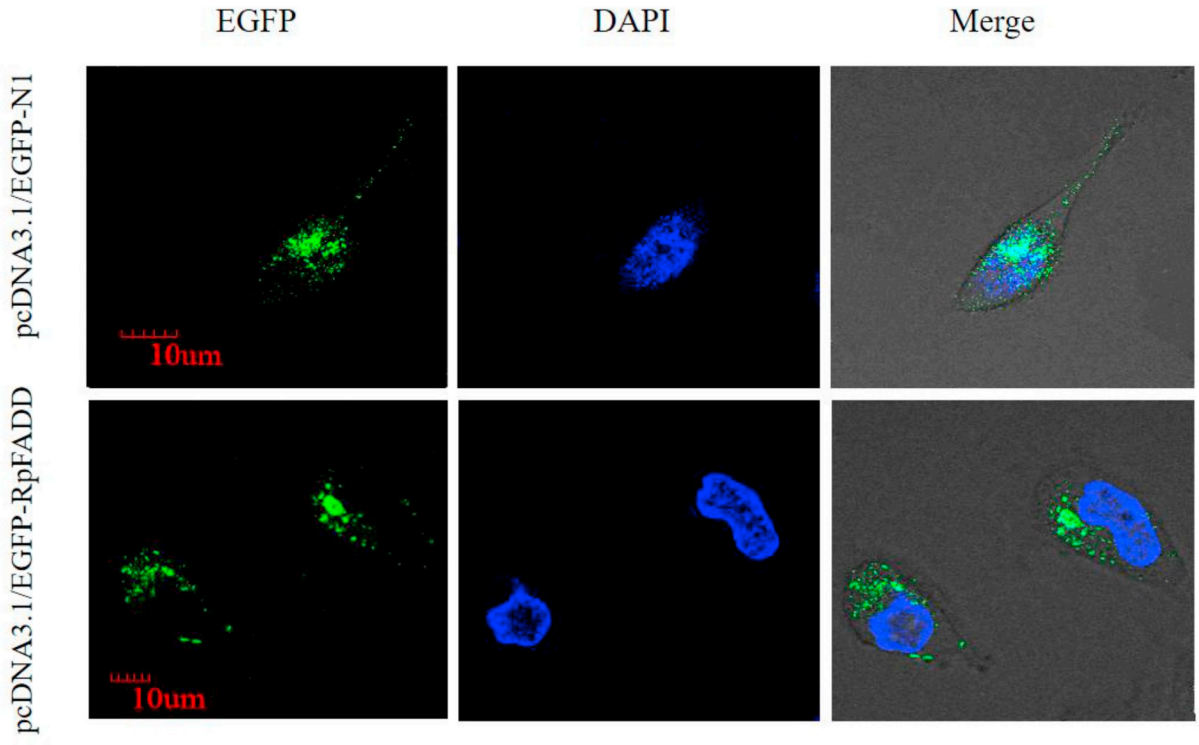

Fig. 8. Subcellular location of RpFADD protein. EGFP staining: left row, DAPI staining: middle row, and EGFP/DAPI staining: right row. The upper panels depict localization of the EGFP control, and the lower panels depict localization of the RpFADD-EGFP protein.

RpFADD expression in the blank and negative control groups, whereas dsRpFADD significantly decreased the expression of RpFADD ($P < 0.01$) (Fig. 5A). Western blotting analysis showed a significant decrease in the abundance of RpFADD protein (Fig. 5B), which was in congruent with the QRT-PCR results. All these results demonstrated that we have successfully knocked down RpFADD in *R. philippinarum*.

In mammalian, FADD usually bind to other signaling molecules containing the death domain like MyD88 to allow IL-1R associated kinase 4 (IRAK-4) to phosphorylate IRAK-1, ultimately causing activation of NF-κB signal pathways [20]. Upon signaling, IκB kinase (IKK) activates transforming growth factor-β-activated kinase 1 (TAK1) and then activates the IκB kinase complex. Moreover, IκB proteins are rapidly phosphorylated by an active IKK complex and subsequently undergo proteasomal degradation, which liberates free NF-κB dimers that can enter the nucleus to promote gene transcription [21–23]. In the present study, the transcript levels of RpIKK, RpTAK1 and RpNF-κB were down-regulated at 12 h ($P < 0.01$), but not RpIκB in dsRpFADD-treated group (Fig. 6). Moreover, the presence of *V. anguillarum* and *M. luteus* extremely significantly increased the expression of RpIKK, RpTAK1, RpNF-κB, RpDefensin and RpMacin ($P < 0.01$) (Fig. 7). However, knockdown of RpFADD expression significantly reduced the expression of these genes ($P < 0.01$) with the exception of RpIκB (Fig. 7). The reason might lie in that down-expression of RpTAK1 and RpIKK blocked the degradation of IκB protein by phosphorylation and ubiquitination, and finally increasing the expression of IκB [24]. Those above results showed that down-regulation of the endogenous expression of RpFADD significantly inhibit the activation of NF-κB signal pathways. In addition, the expression levels of two immune-related antimicrobial peptide genes RpDefensin and RpMacin were extremely significantly decreased compared to that of the blank and control groups at 72 h ($P < 0.01$) (Fig. 7). Similarly, when knockdown FADD in mosquitoes, the mRNA levels of antibacterial peptides (e.g. cecropin and defensin) were also significantly reduced [15]. These results suggested that RpFADD was required for the expression of AMP genes, and also for the immune responses against both *M. luteus* and *V. anguillarum* challenge.

3.6. Subcellular location of RpFADD and its ability to induce cell death

Subcellular location results revealed that the fusion RpFADD-2-EGFP expression region (green) tightly surrounded the nucleus (blue), demonstrating that RpFADD is a cytosolic protein (Fig. 8). It was suggested that FADD is involved in the regulation of activated caspase-3 translocation from cytoplasm to nucleus in apoptotic cells [25]. Quantitative analysis by flow cytometry showed that, compared to control cells, the cells transfected with pcDNA3.1/EGFP-RpFADD plasmids exhibited higher percentage of apoptosis (17.1%, $P < 0.01$, Fig. 9). The induced expression of FADD might activate extrinsic pathway responsible for apoptotic cell death [2], which usually performed by binding with the procaspase-8 death domain to form the DISC [26,27]. Once procaspase-3 is activated by the formation of DISC, capsase-3 is activated to induce apoptosis [28–30].

In conclusion, a RpFADD gene was identified from manila clam *R. philippinarum*. Especially, RpFADD was highly expressed in hemocytes,

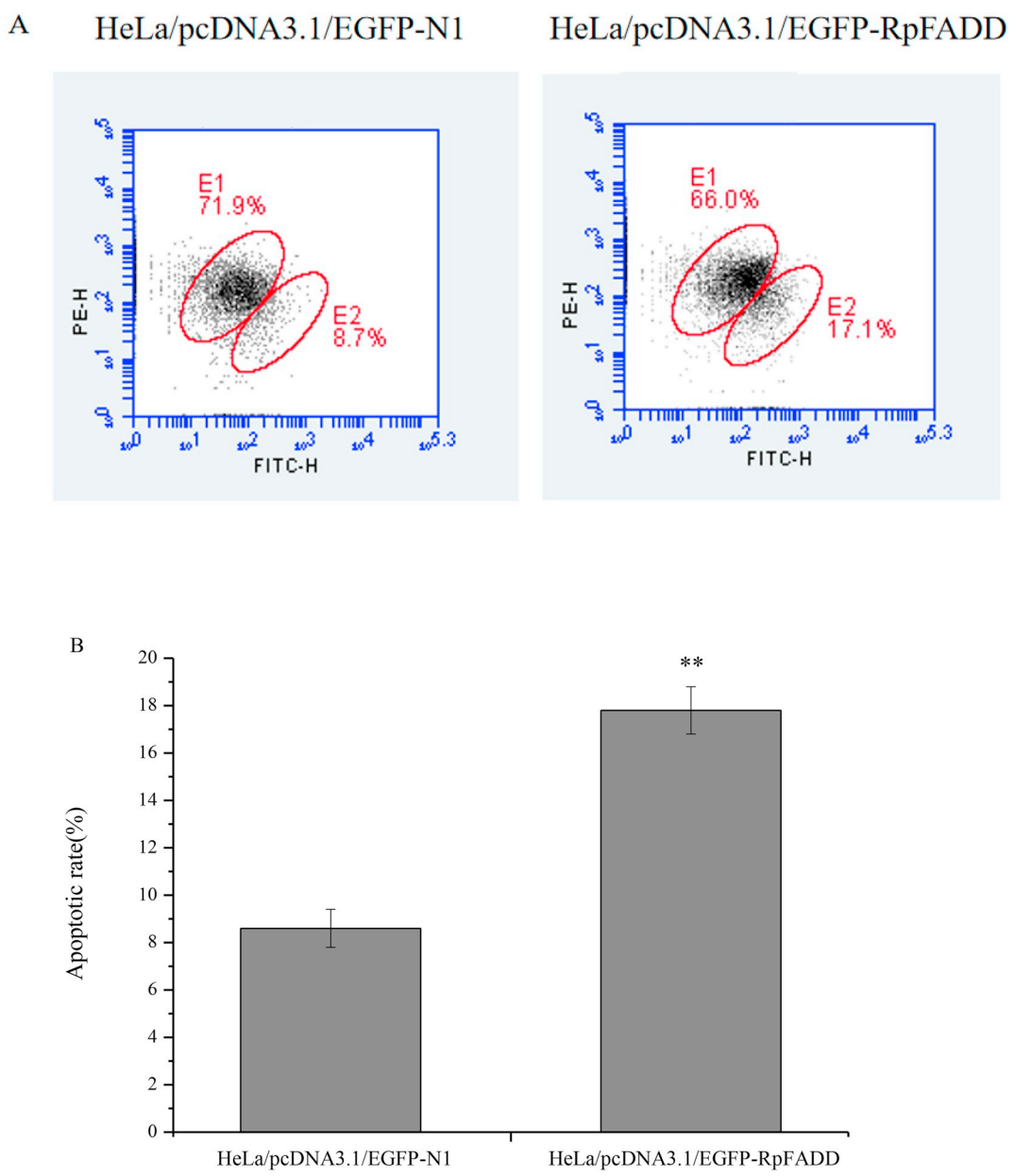

Fig. 9. Roles of RpFADD in apoptosis. Flow cytometry analysis of cell apoptosis rate in HeLa cells (A and B). The values are showed as mean ± S.D. (N = 3). (*: $P < 0.05$, **: $P < 0.01$).

supporting its involvement in the immune response against bacterial infection. We also found that RpFADD is primarily localized in the cell cytoplasm and involved in apoptosis. These results provided clues to clarify that RpFADD was an important molecule involved in the innate immunity of *R. philippinarum*.

Acknowledgments

This research was supported by grants from the Strategic Priority Research Program of the Chinese Academy of Sciences (XDA23050303), the National Natural Science Foundation of China (No. 41806196), and the Youth Innovation Promotion Association CAS (2016196).

References

[1] J.P. Medema, C. Scaffidi, F.C. Kischkel, A. Shevchenko, M. Mann, P.H. Krammer, et al., FLICE is activated by association with the CD95 death-inducing signaling complex (DISC), EMBO J. 16 (1997) 2794–2804.

[2] A.M. Chinnaiyan, K. Orourke, M. Tewari, V.M. Dixit, Fadd, a novel death domain-containing protein, interacts with the death domain of Fas and initiates apoptosis, Cell 81 (1995) 505–512.

[3] C. Scaffidi, J. Volkland, I. Blomberg, I. Hoffmann, P.H. Krammer, M.E. Peter, Phosphorylation of FADD/MORT1 at serine 194 and association with a 70-kDa cell cycle-regulated protein kinase, J. Immunol. 164 (2000) 1236–1242.

[4] B.C. Barnhart, J.C. Lee, E.C. Alappat, M.E. Peter, The death effector domain protein family, Oncogene 22 (2003) 8634–8644.

[5] E.J. Jeong, S. Bang, T.H. Lee, Y.I. Park, W.S. Sim, K.S. Kim, The solution structure of FADD death domain - structural basis of death domain interactions of Fas and FADD, J. Biol. Chem. 274 (1999) 16337–16342.

[6] H. Berglund, D. Olerenshaw, A. Sankar, M. Federwisch, N.Q. McDonald, P.C. Driscoll, The three-dimensional solution structure and dynamic properties of the human FADD death domain, J. Mol. Biol. 302 (2000) 171–188.

[7] P.E. Carrington, C. Sandu, Y.F. Wei, J.M. Hill, G. Morisawa, T. Huang, et al., The structure of FADD and its mode of interaction with procaspase-8, Mol. Cell 22 (2006) 599–610.

[8] M.H. Werner, C.W. Wu, C.M. Walsh, Emerging roles for the death adaptor FADD in death receptor avidity and cell cycle regulation, Cell Cycle 5 (2006) 2332–2338.

[9] S.H. Kaufmann, M.O. Hengartner, Programmed cell death: alive and well in the new millennium, Trends Cell Biol. 11 (2001) 526–534.

[10] F. Leulier, A. Rodriguez, R.S. Khush, J.M. Abrams, B. Lemaitre, The Drosophila caspase Dredd is required to resist Gram-negative bacterial infection, EMBO Rep. 1

(2000) 353–358.
[11] J.A. Hoffmann, J.M. Reichhart, Drosophila immunity, Trends Cell Biol. 7 (1997) 309–316.
[12] X. Zhang, S.Q. Zang, C. Li, J.G. Wei, Q.W. Qin, Molecular cloning and characterization of FADD from the orange-spotted grouper (*Epinephelus coioides*), Fish Shellfish Immunol. 74 (2018) 517–529.
[13] R.J. Yang, J.Y. Li, X. Gao, Z.H. Zhao, L.P. Zhang, H.J. Gao, et al., Fas-associated death domain (FADD) mediated activation of a apoptosis program in bovine follicular granulosa cells, J. Anim. Vet. Adv. 10 (2011) 1994–2003.
[14] F.M.M.T. Marikar, D.Y. Ma, J.Q. Ye, B. Tang, W.J. Zheng, J. Zhang, et al., Expression of recombinant human FADD, preparation of its polyclonal antiserum and the application in immunoassays, Cell. Mol. Immunol. 5 (2008) 471–474.
[15] D.M. Cooper, C.M. Chamberlain, C. Lowenberger, F.A.D.D. Aedes, A novel death domain-containing protein required for antibacterial immunity in the yellow fever mosquito, *Aedes aegypti*, Insect Biochem. Mol. 39 (2009) 47–54.
[16] D.L. Yang, Q. Wang, R.W. Cao, L.Z. Chen, Y.L. Liu, M. Cong, et al., Molecular characterization, expression and antimicrobial activities of two c-type lysozymes from manila clam *Venerupis philippinarum*, Dev. Comp. Immunol. 73 (2017) 109–118.
[17] K.J. Livak, T.D. Schmittgen, Analysis of relative gene expression data using real-time quantitative PCR and the 2(T)(-Delta Delta C) method, Methods 25 (2001) 402–408.
[18] Z.Y. Tang, M.J. Sheng, Y.X. Qi, L.Y. Wang, D.Y. He, Metformin enhances inhibitive effects of carboplatin on HeLa cell proliferation and increases sensitivity to carboplatin by activating mitochondrial associated apoptosis signaling pathway, Eur. Rev. Med. Pharmacol. 22 (2018) 8104–8112.
[19] L.L. Wang, X.R. Song, L.S. Song, The oyster immunity, Dev. Comp. Immunol. 80 (2018) 99–118.
[20] C.A. Janeway, R. Medzhitov, Innate immune recognition, Annu. Rev. Immunol. 20 (2002) 197–216.
[21] Q. Yang, Z. Yang, H.J. Li, Molecular characterization and expression analysis of an inhibitor of NF-kappa B (I kappa B) from Asiatic hard clam *Meretrix meretrix*, Fish Shellfish Immunol. 31 (2011) 485–490.
[22] T.J. Green, A.C. Barnes, Inhibitor of REL/NF-B-K is regulated in Sydney rock oysters in response to specific double-stranded RNA and *Vibrio alginolyticus*, but the major immune anti-oxidants EcSOD and Prx6 are non-inducible, Fish Shellfish Immunol. 27 (2009) 260–265.
[23] C.K. Mu, Y.D. Yu, J.M. Zhao, L.L. Wang, X.Y. Song, H. Zhang, et al., An inhibitor kappa B homologue from bay scallop *Argopecten irradians*, Fish Shellfish Immunol. 28 (2010) 687–694.
[24] M.S. Hayden, S. Ghosh, NF-kappa B in immunobiology, Cell Res. 21 (2011) 223–244.
[25] S. Kamada, U. Kikkawa, Y. Tsujimoto, T. Hunter, Nuclear translocation of caspase-3 is dependent on its proteolytic activation and recognition of a substrate-like protein (s), J. Biol. Chem. 280 (2005) 857–860.
[26] M.P. Boldin, T.M. Goncharov, Y.V. Goltsev, D. Wallach, Involvement of MACH, a novel MORT1/FADD-interacting protease, in Fas/APO-1- and TNF receptor-induced cell death, Cell 85 (1996) 803–815.
[27] M. Muzio, A.M. Chinnaiyan, F.C. Kischkel, K. ORourke, A. Shevchenko, J. Ni, et al., FLICE, a novel FADD-homologous ICE/CED-3-like protease, is recruited to the CD95 (Fas/APO-1) death-inducing signaling complex, Cell 85 (1996) 817–827.
[28] I. Lavrik, A. Krueger, I. Schmitz, S. Baumann, H. Weyd, P.H. Krammer, et al., The active caspase-8 heterotetramer is formed at the CD95 DISC, Cell Death Differ. 10 (2003) 144–145.
[29] M. Muzio, B.R. Stockwell, H.R. Stennicke, G.S. Salvesen, V.M. Dixit, An induced proximity model for caspase-8 activation, J. Biol. Chem. 273 (1998) 2926–2930.
[30] I.N. Lavrik, A. Golks, P.H. Krammer, Caspases: pharmacological manipulation of cell death, J. Clin. Investig. 115 (2005) 2665–2672.